ANL/NE-12/12

Argonne NATIONAL LABORATORY

Laser Welding and Post Weld Treatment of Modified 9Cr-1MoVNb Steel

Nuclear Engineering Division

About Argonne National Laboratory

Argonne is a U.S. Department of Energy laboratory managed by UChicago Argonne, LLC under contract DE-AC02-06CH11357. The Laboratory's main facility is outside Chicago, at 9700 South Cass Avenue, Argonne, Illinois 60439. For information about Argonne, see www.anl.gov.

Availability of This Report

This report is available, at no cost, at http://www.osti.gov/bridge. It is also available on paper to the U.S. Department of Energy and its contractors, for a processing fee, from:

U.S. Department of Energy
Office of Scientific and Technical Information
P.O. Box 62
Oak Ridge, TN 37831-0062 phone
(865) 576-8401
fax (865) 576-5728
reports@adonis.osti.gov

ANL/NE-12/12

Laser Welding and Post Weld Treatment of Modified 9Cr-1VNb Steel

by
Zhiyue Xu
Nuclear Engineering Division, Argonne National Laboratory

September 30, 2008

Summary

Laser welding and post weld laser treatment of modified 9Cr-1MoVNb steels (Grade P91) were performed in this preliminary study to investigate the feasibility of using laser welding process as a potential alternative to arc welding methods for solving the Type IV cracking problem in P91 steel welds. The mechanical and metallurgical testing of the pulsed Nd:YAG laser-welded samples shows the following conclusions:

1. Both bead-on-plate and circumferential butt welds made by a pulsed Nd:YAG laser show good welds that are free of microcracks and porosity. The narrow heat affected zone has a homogeneous grain structure without conventional soft hardness zone where the Type IV cracking occurs in conventional arc welds.
2. The laser weld tests also show that the same laser welder has the potential to be used as a multi-function tool for weld surface remelting, glazing or post weld tempering to reduce the weld surface defects and to increase the cracking resistance and toughness of the welds.
3. The Vicker hardness of laser welds in the weld and heat affected zone was 420 – 500 HV with peak hardness in the HAZ compared to 240 HV of base metal. Post weld laser treatment was able to slightly reduce the peak hardness and smoothen the hardness profile, but failed to bring the hardness down to below 300 HV due to insufficient time at temperature and too fast cooling rate after the time. Though optimal hardness of weld made by laser is to be determined for best weld strength, methods to achieve the post weld laser treatment temperature, time at the temperature and slow cooling rate need to be developed.
4. Mechanical testing of the laser weld and post weld laser treated samples need to be performed to evaluate the effects of laser post treatments such as surface remelting, glazing , re-hardening, or tempering on the strength of the welds.

Table of Contents

Laser Welding and Post Weld Treatment of Modified 9Cr-1MoVNb Steel

Zhiyue Xu
Nuclear Engineering Division, Argonne National Laboratory, IL 60439, USA

Introduction

When most of the experimental and prototype sodium fast rectors (SFR) were built in the 1960s and 70s, 2.25Cr-1Mo steels (Grade 22 or P22) were used for key components such as steam generators. Today high chromium ferritic steels such as modified 9Cr-1MoVNb steels (Grade 91 or P(T) 91) and 9Cr-1Mo-1.8WVNb (NF616 or P/T92) are the leading candidate materials for constructing SFR components due to their enhanced properties over traditional power plant steel, such as 2.25Cr-1Mo and 300-series austenitic stainless steels. Figure 1 shows the evolution of the 9 – 12 Cr ferritic heat resistant steels and their creep rupture strength at 600 ^{0}C [1]. Figure 2 [2] illustrates a comparison of wall thickness for various alloys for a given elevated temperature, pressure and allowable strength. Note that nearly a 2:1 reduction in wall thickness (61mm versus 132mm) is possible when modified Grade 91 or P91 is used in place of P22 material. The material provides an increase of 44 to 170% in allowable strength in the 510 ^{0}C (950 ^{0}F) to 593^{0}C (1100 ^{0}F) temperature range. The oxidation limit is also 38 ^{0}C (100 ^{0}F) above typical Grade 22 materials. Grade 91 also offers higher allowable strengths over type 304H up to 610 ^{0}C (1130 ^{0}F). However, to obtain such superior properties in the alloy, considerable care during welding is required to assure acceptable long-term properties.

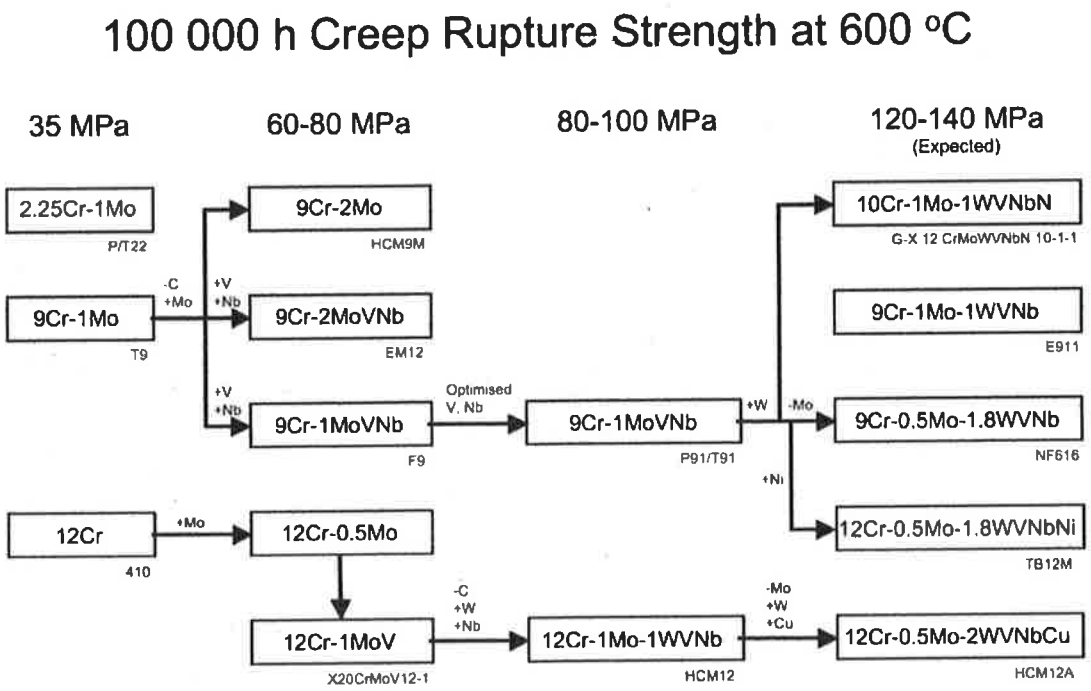

Figure 1. Evolution of 9 – 12 Cr ferritic heat resistant steels [1].

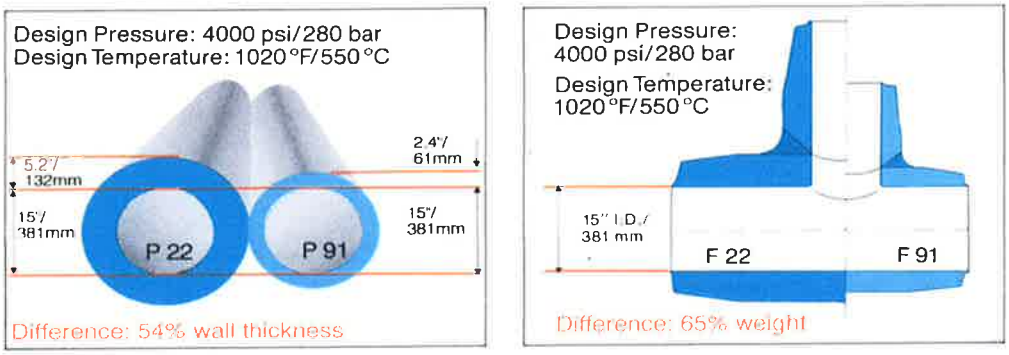

Figure 2. Comparison of thickness and weight using P91 versus P22 steel [2]

Conventional arc welding of P91 generally requires preheating the joint, maintaining interpass temperatures, hydrogen bakes, and post weld heat treatment (PWHT). A typical temperature schedule for a welded joint in P91 steel is presented in Figure 3. During the PWHT, the heating rate, treatment temperature, time at temperature, and the cooling rate all have to be carefully controlled in order to produce the proper microstructure and properties of the welds.

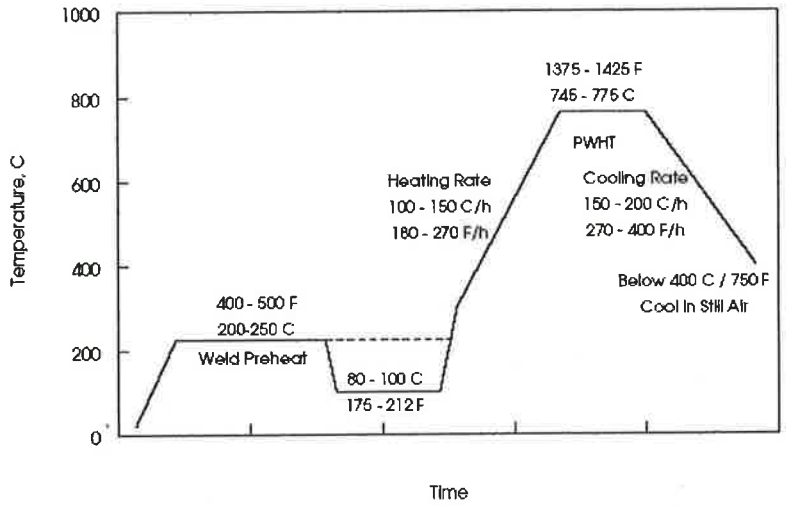

Figure 3. Typical temperature schedule for welded joints in P91 steel [3].

Conventional welding processes for joining P91 steel include flux cored arc welding (FCAW), gas metal arc welding (GMAW), gas tungston arc welding (GTAW), submerged arc welding (SAW), and shielded metal arc welding (SMAW). Figure 4 a) represents a cross-section through a welded joint in a thick walled P91 ferritic steel pipe. Given its ability to make high quality welds, GTAW is used to complete the root pass, which, because it is the first physical joint between the component plates, is particularly vulnerable to contraction strains. The same GTAW can be used to complete the joint but manual metal arc welding (MMAW) is often used in complex joints, or high productivity processes such as flux cored arc welding and submerged arc welding for deep welds. Welding wires such as TGS-9CB (Kobe Steel) are used to make the joints. For dissimilar welded joints between modified 9Cr-1Mo steel and austenitic steel such as SUS 304-HP,

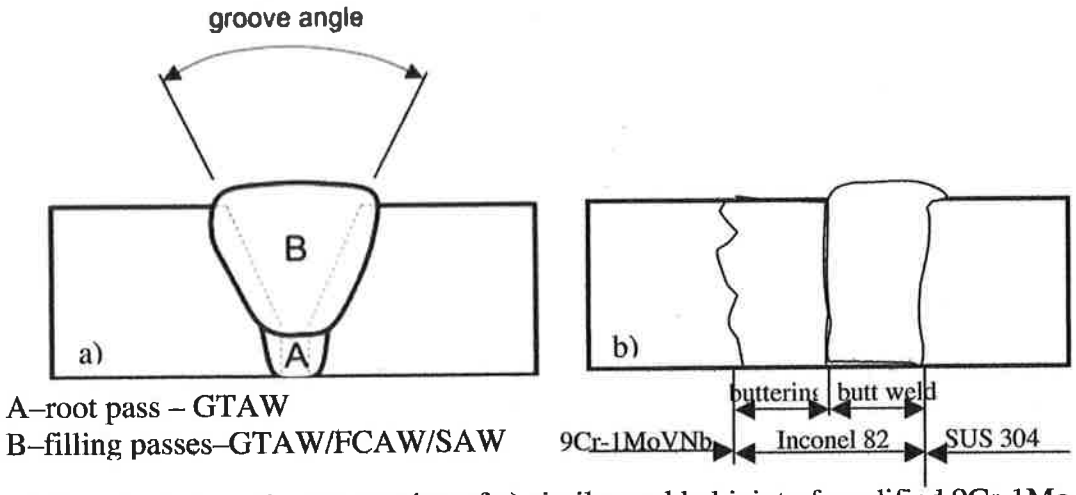

Figure 4. Schematic presentation of a) similar welded joint of modified 9Cr-1Mo ferritic steel and b) a dissimilar welded joint between modified 9Cr-1Mo steel and austenitic steel [3, 4].

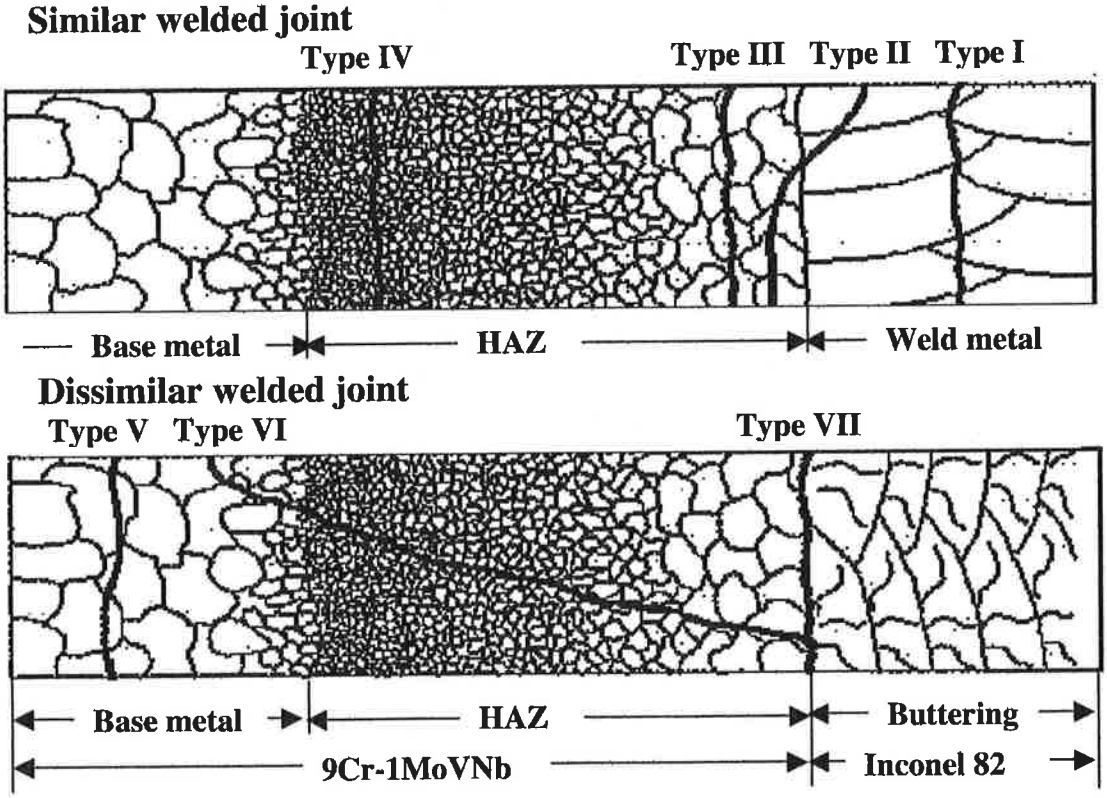

Figure 5. Schematic showing fracture type of welded joints [4].

the modified 9Cr-1Mo steel plate is first buttered using weld metals such as Inconel 82 (Wel-82, Nippon Welding Rod). Then it is butt welded with the SUS 304-HP steel plate using the same type of welding wire. GATW is the usual welding method for both buttering and butt welding. A cross-sectional view of such a dissimilar welded joint is shown in Figure 4 b).

Welds are more subject to failure than the parent material because of the possibility of surface irregularities and fissures, because of residual stresses, and because of local variations in material structures and compositions. The weld-zone fracture types of the similar and dissimilar welded joints are schematically illustrated in Figure 5 [4]. The rupture types are classified based on the rupture location in the weld zone of similar welded joints. Type I has rupture due to cracks generated only in the weld metal. Type II cracks span across the weld metal and into the coarse region of the HAZ. Type III cracks lie entirely in the coarse region of the HAZ. Type IV cracks lie entirely in the fine-grained region of the HAZ. However, the rupture locations for dissimilar welded joints are different. Three more types are added to the classifications. Type V has rupture due to cracks generated only in the 9Cr-1MoVNb steel. Type VI cracks span across the region from the interface of the 9Cr-1MoVNb steel HAZ and Inconel 82 to the 9Cr-1MoVNb steel HAZ and the base metal of 9Cr-1MoVNb steel, and Type VII cracks are at the interface between the 9Cr-1MoVNb steel HAZ and Inconel 82.

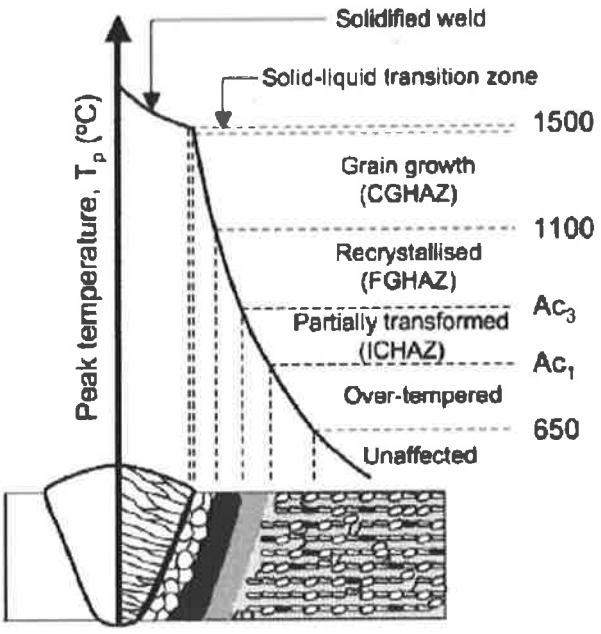

Figure 6. Schematic representation of microstructures developed in HAZ as function of peak temperature during welding of P91 steel.

One of the most significant problems with conventional welding of modified 9Cr1Mo steel is the premature Type-IV cracking failure of the weldment, which occurs because of the local gradients of microstructure in the HAZ of the welds. The microstructural regions of a weld are illustrated in Figure 6 and classified as follows:

1. course grain region (CGHAZ);
2. fine grain region (FGHAZ);
3. intercritical region (ICHAZ), and
4. over tempered region.

The Type IV failures occur at the FGHAZ region, adjacent to the ICHAZ as shown in Figure 7. It is a form of cracking where there is an enhanced rate of creep void formation in the fine grained and inter-critically annealed HAZ of the weld, leading to early failure when compared with creep tests on the unwelded steel.

Figure 7. Type IV failure on the grain boundaries in the fine-grained HAZ in weld joint of modified 9Cr-1Mo steel.

Laser welding has been widely used as an important material joining technology in the auto industry, shipbuilding, aerospace industry, pressure vessels and medical equipment. The small heat affected zone and weld microstructure and surface tailoring ability in laser welding make the process a potential alternative to arc welding methods for solving the Type IV cracking problem in P91 steel welds. The purpose of current study was to preliminarily investigate the effects of laser welding parameters on the structure and microhardness of welds and to evaluate the feasibility of using a laser welding process to produce welds free of Type IV cracking.

Experimental setup

1. Material

The material used in this study was Grade P91 (ASTM A335) steel tube ordered from Tioga Pipe Supply Co. The size of the tube was 1.315" (diameter) x 0.133" (wall thickness) (33.40 X 3.38 mm). The chemical compositions and mechanical properties of the material are listed in Table 1 and Table 2 respectively. The as-received P91 tube was normalized at 1940 ^{0}F for 20 minutes and then tempered at 1436 ^{0}F for 60 minutes. The as-received microstructure of the tube is shown in Figure 8, which shows tempered grain structures of around 10 μm.

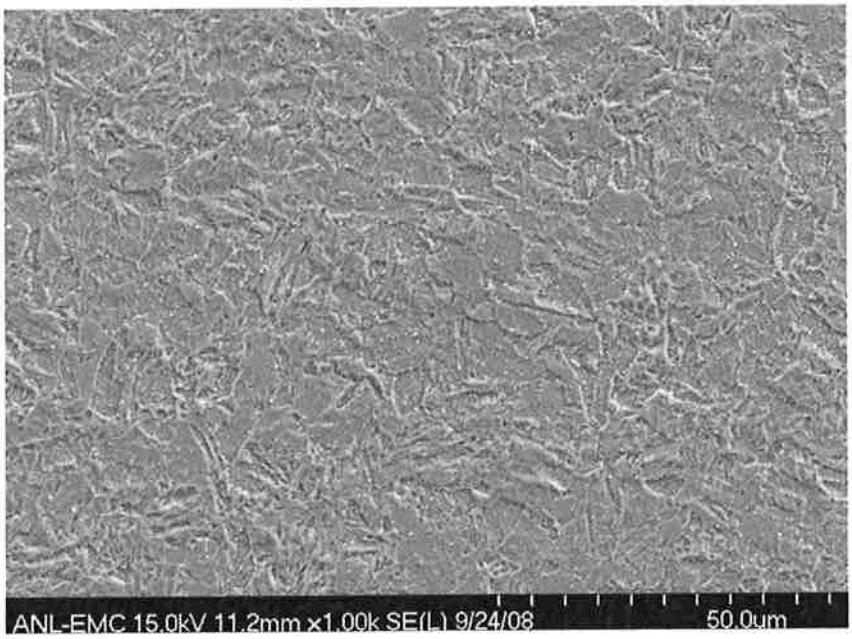

Figure 8. SEM photograph of as-received microstructure of P91 tube.

Table 1. Chemical analysis (%) of P91 steel from Tioga Pipe Supply Co.

C	Si	Mn	P	S	Cr	Mo	Ni	Al	Nb	V	N
0.10	0.36	0.41	0.011	0.001	8.56	1.03	0.10	0.009	0.10	0.24	0.056

Table 2. Mechanical properties of P91 steel at room temperature

Width, mm	Thickness, mm	Section area, mm^2	Yield strength, psi	Tensile strength, psi	Elongation, %	Rockwell C hardness
19.00	3.55	72.07	77496	106691	26	<= 22

2. Weld samples

Two different welds shown in black in Figure 9 were made. The bead-on-plate (BOP) welds shown in Figure 9a were made on a section of the tube by moving the tube

under a vertical laser beam. The circumferential butt weld shown in Figure 9b, used to join two short tubes was made by rotating the tube under a vertical laser beam. The two tubes to be welded were held together during the laser welding by a fixture schematically shown in Figure 10. The fixture simply includes a bolt (green) through the center of the two tubes and two nuts (yellow) to clamp the tubes together. Belleville disk spring washers were used at both ends of the nuts to provide some adjustment to potential thermal expansion from the welding and resultant heating.

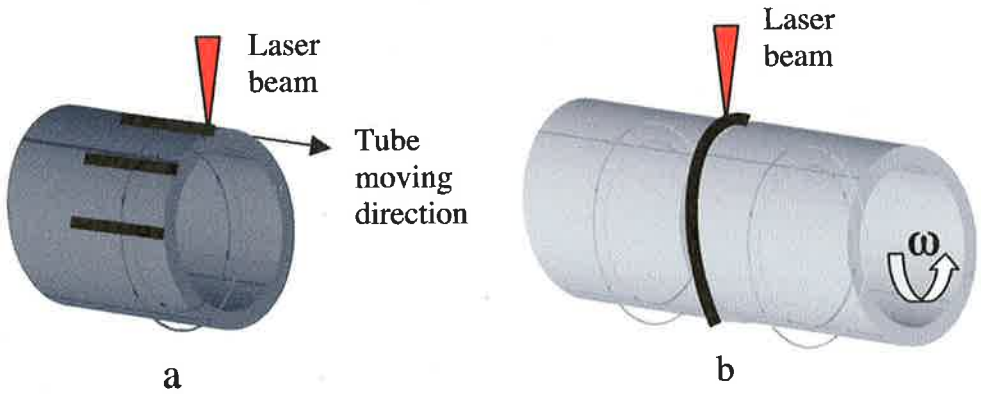

Figure 9. Laser welding sample design: a. BOP welds and b. circumferential butt weld.

Figure 10. Schematic showing fixture design for circumferential butt welding.

3. Laser parameter and welding procedure

The laser used was a 1.6 kW pulsed Nd:YAG laser with fiber optic beam delivery. The key technical specifications of the laser are:

Laser average power:	1600 W
Pulse width:	0.1 – 10 ms
Maximum pulse rep rate:	800 Hz
Maximum peak power:	32 000 W
Maximum pulse energy:	100 J

The optics used include a 128 mm focal length collimating lens and a spherical convex Gradium lens with a focal length of 77 mm. The size of the focused beam was

1 mm, which was positioned 1 mm below the surface of the workpiece. A leading cover gas jet of argon at 60 SCFH aimed at the welding spot to provide the means of anti-oxidation and a cross flow air knife of nitrogen at 200 SCFH were used to prevent lens contamination from spatter during welding.

First, a series of BOP welds were produced with different laser parameter combinations to screen the best combination. The parameters screened are listed in Table 4. Then the optimal parameter combinations (Weld #7 in Table 4) were used to produce the circumferential butt welds. Post weld laser treatments (PWLT) were also applied to the welds to evaluate their effects on weld properties. For PWLT, the laser beam size was increased to 3.5 mm, 4 mm, and 5 mm. To monitor the effect of PWLT, the temperature of the internal surface of tube directly under the laser beam was measured during the PWLT. The PWLT parameter and resultant temperatures are listed in Table 5. The parameters used for post weld laser treatment of the welds and the internal surface temperatures are listed in Table 6.

4. Weld characterization

Metallurgical samples of cross sections of the BOP and butt welds with or without post weld laser treatment were prepared. The microstructures of weld beads, heat affected zone and base metals were analyzed using an optical microscope and scanning electron microscope. The microhardness profiles were measurement across the welds at different weld depths.

Table 4. Laser parameters for screening tests

Weld #	Laser peak power, W	Pulse width, ms	Pulse rep rate, Hz	Beam travel speed, mm/s	Notes
1	16000	1	100	1.5	Cutting
2	8000	1	200	3.0	Dropout
3	8000	1	200	10	undercut
4	8000	1	200	6.0	dropout
5	6000	1.33	200	6.0	Good
6	5000	1.6	200	6.0	Good
7	5000	1.6	200	5.0	Good

Table 5. Temperatures of internal surface of the tube directly under the beam

PWLT #	Laser schedule	Beam travel speed, cm/s	Beam size, mm	Bottom side temperature ^{0}C	# of passes
1	E6L1R240	0.3	5	580	1
2	E6L1R240	0.5	5	324	1
3	E5L1R240	0.5	5	266	1
4	E5L1R240	0.5	5	268	2
5	E5L1R240	0.5	4	315	1

Table 6. Post weld laser treatment parameters and associated internal surface temperature

Measurement #	Laser schedule	Beam travel speed, cm/s	Beam size, mm	Bottom side temperature ^{0}C	# of passes
1	E8L1R200	0.1	3.5	800	1
2	E6L1R200	0.3	3.5	560	1
3	E5L1R200	0.3	3.5	475	1
4	E5L1R240	0.3	4	487	1
5	E5L1R240	0.5	4	331	1
6	E4L1R300	0.5	4	219	1

Results and Discussions

1. Bead-on-plate welds for parameter screening tests

Microstructures

The cross-section microstructures of the six bead-on-plate welds, Weld # 2 – 7 in Table 4 of the parameter screening tests, are shown in Figure 11. The laser beam with the highest peak power (Weld #1 in Table 4) produced a cutting rather than a weld, and therefore is not shown in Figure 11. The weld bead (W), heat affected zone (H), and base metal (B) are clearly shown by the etched photos. All welds are free of cracks and porosity. The weld penetrations measured are listed in Table 7. Weld # 2 and #4 show full penetration welds through the tube wall thickness of 3.38 mm but melted metal dropped out at the bottom of the welds, which indicates over-applied laser energy. The slight tilting of the weld bead # 6 and 7 shown in Figure 11 was due to the 5 degree of laser beam titling from the vertical. Weld # 7 shows the deepest penetration among the rest of the welds and good weld bead profile and was selected for the circumferential butt welds. Further mechanical and metallurgical analysis and as well as post weld laser treatment of the welds were done on weld # 7.

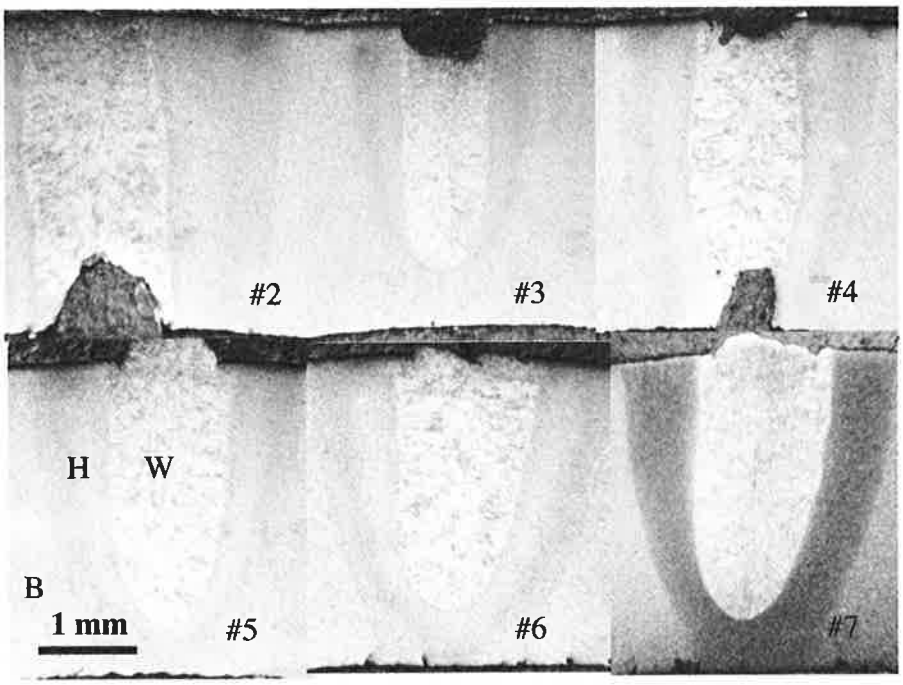

Figure 11. Cross-section optical microscope photographs of bead-on-plate welds in Grade P91 steel tube made by pulsed Nd:YAG laser with different laser parameters.

Table 7. Weld penetrations of welds in parameter screening tests

Weld #	2	3	4	5	6	7
Depth, mm	Full, 3.38	2.56	Full, 3.38	2.74	2.68	2.83

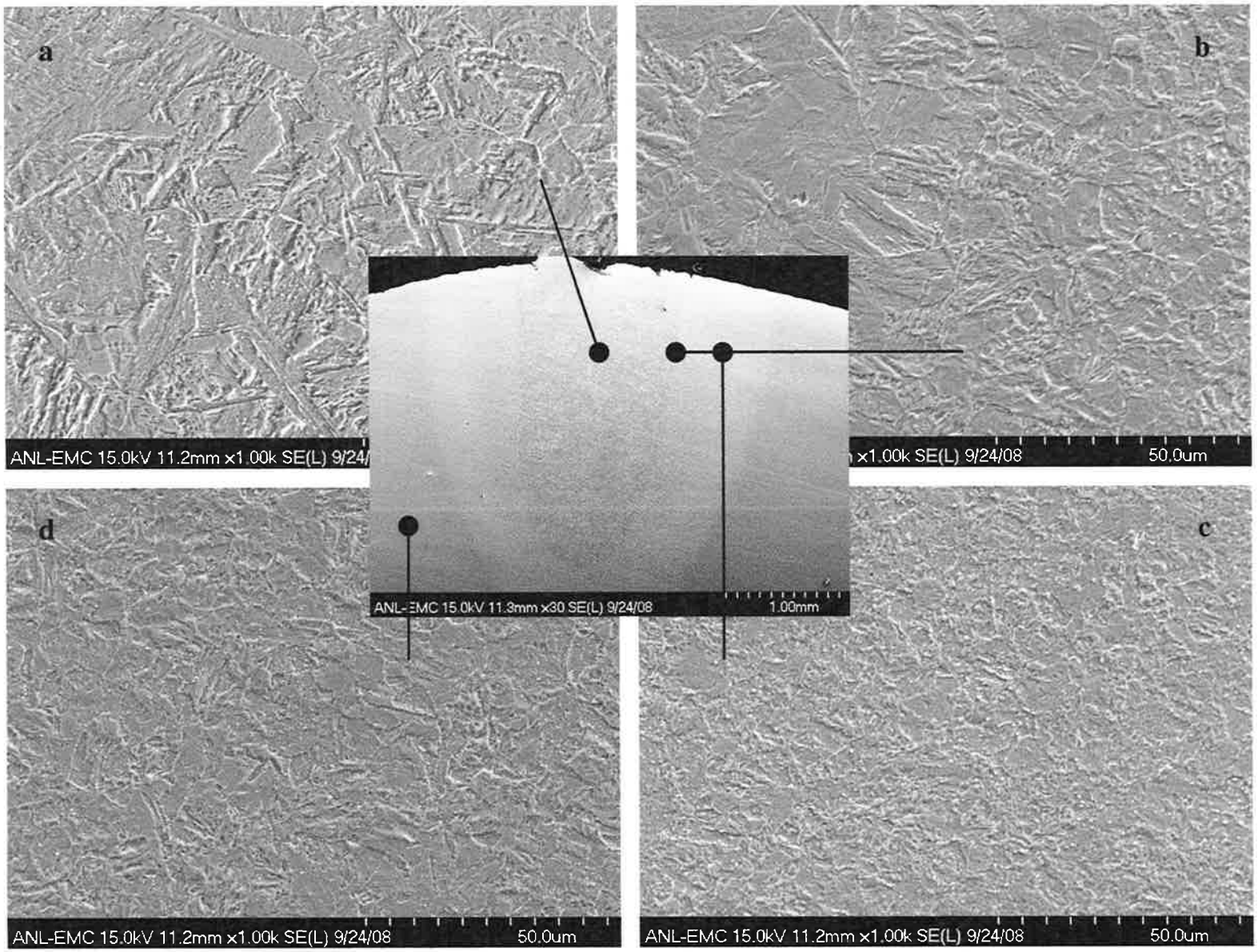

Figure 12. SEM micrographs of a) weld zone, b) weld to HAZ transition zone, c) heat affected zone, and d) base metal.

The SEM micrographs of weld #7 are shown in Figure 12, all of which were taken at a magnification of 1K. The picture at the center is a 30 X full view of the Weld #7. The microstructure of weld zone (Figure 12a) is comprised of elongated grains with a column-like structure with grain sizes as large as 40 μm along the longitudinal axis of the grains. Structure transition from weld zone to HAZ is clearly shown in Figure 12b, where the grain sizes reduce from 40 μm in weld zone to 5 - 10 μm into HAZ. Figure 12c shows the microstructure in the heat-affected zone with grain size around 5 μm. The microstructure of base metal is shown in Figure 12d with the grain size of 10 μm. Clear coarse and fine heat affected zone structures normally shown in conventional arc welds are not seen in the laser welded sample.

Microhardness profiles

Microhardness profiles of Weld #7 are shown in Figure 13. The weld and HAZ have Vickers hardness above 400 compared to 230 for the base metal. The peak hardness was in the HAZ of the weld for all three profiles. The highest peak hardness occured in HAZ at the bottom of the weld. This could be that the material at the bottom of the weld HAZ was closer to the surface and cooled faster than the rest of the weld area.

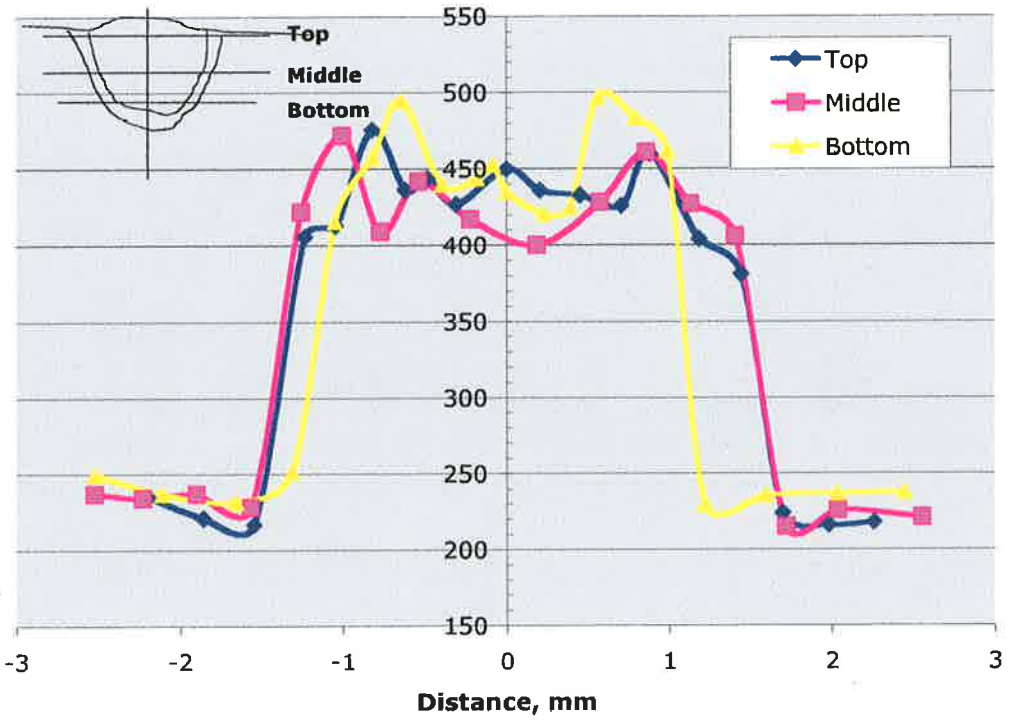

Figure 12. Microhardness profiles of BOP Weld #7 at different weld depths across weld bead, HAZ, and base metal.

2. Circumferential butt weld

Microstructures

A cross-section full view of the butt weld is shown in Figure 13, which presents the similar structure characteristics to the BOP weld. The seam that originally existed at the joint before welding was completely closed and disappeared.

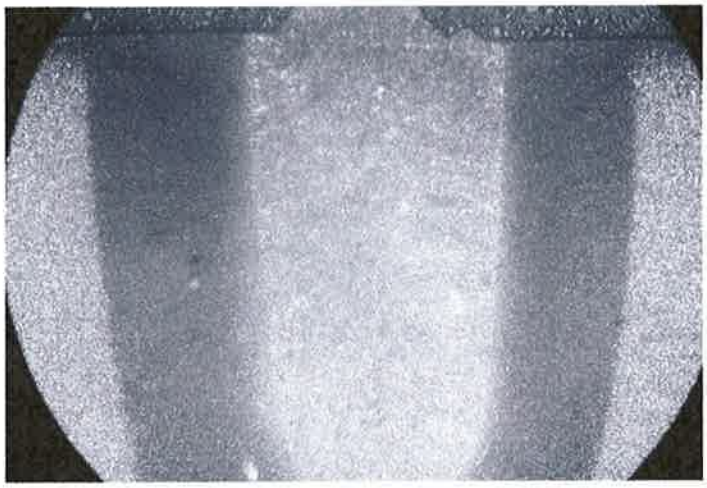

Figure 13. Cross-section view of circumferential butt weld.

Microhardness profiles

Microhardness profiles of the butt weld at three different cross sections located along the weld circumference and at the middle of the weld depth are shown in Figure 14. The average Vickers hardness in the weld zone and HAZ was around 450 and again the peak hardness as high as 500 was found in the HAZ.

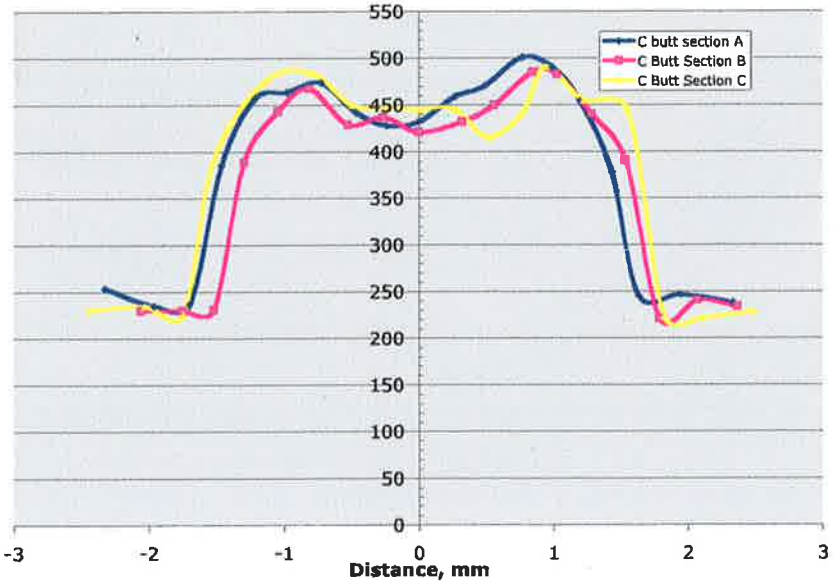

Figure 14. Hardness profile of the circumferential butt weld.

3. Post weld laser treatment

The same laser used to make the weld can be applied to the weld again to do the following:

- Reheat the weld for structure modification and residual stress release,
- Make shallow weld surface remelting for smoothening the weld surface and getting rid of crevices, and
- Create a surface glazing layer of the weld for high corrosion and wear resistance,

During this preliminary study, post weld laser treatments of the welds at different process parameters were carried out (Table 6) and microhardness profiles of the treated welds were measured. Cross-section full views of two of the post weld laser treated weld samples are shown in Figure 15. The different regions on the weld are labeled as follows:

M: new melted surface
W: weld zone
OH: old heat affected zone
NH: new heat affected zone
B: base metal

The depth of the new melted surface layer and new heat affected zone of PWLT can be tailored by adjusting laser treatment parameters. This is shown in the PWLT samples in Figure 15. The PWLT#1 made at high laser energy and slower beam travel speed (3 mm/s) shows a much deeper and wider post weld treatment zone than the PWLT #2 does at same laser energy and faster travel speed (5 mm/s).

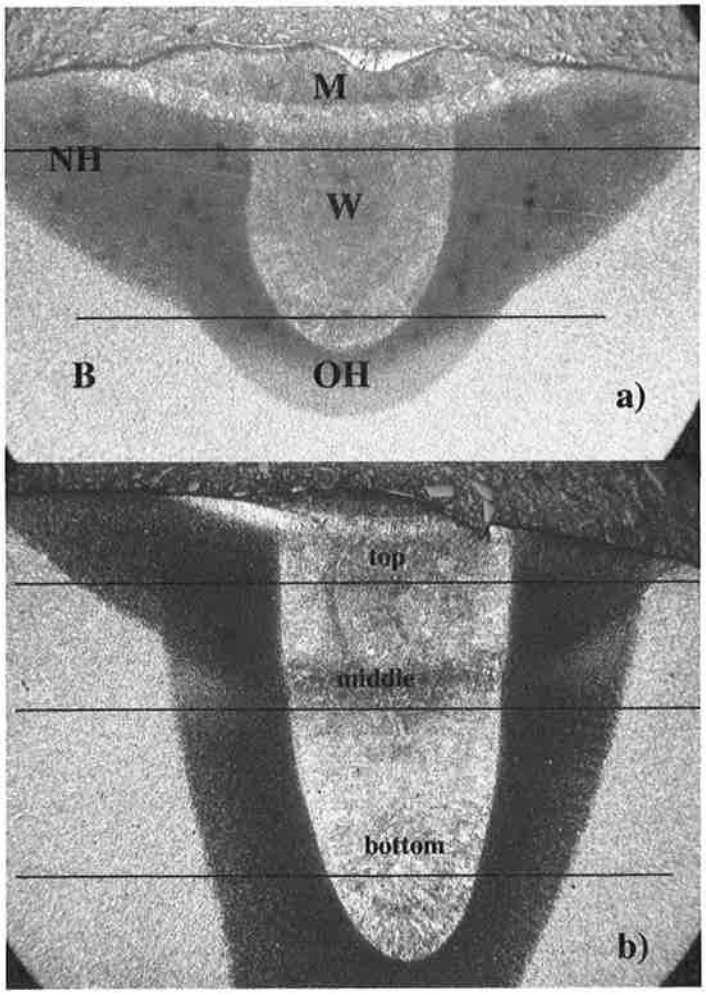

Figure 15. Cross section view of post weld laser treated weld. a) PWLT # 1 and b) PWLT # 2.

The microhardness profiles measured along the horizontal lines in Figure 15 are shown in Figures 16 and 17. The hardness profile at the top of the PWLT#1, made at high laser energy input due to the slower beam travel speed, presents a widened high hardness region and slightly reduced the peak hardness below 500. But at bottom of the weld, the hardness profile barely changed due to the temperature the

bottom reached was low. The same is true for the hardness profiles of the PWLT #2, made at smaller laser energy input due to higher beam travel speed, which do not show significant difference from the profiles of as-laser-welded. To obtain the proper toughness of the weld, guidelines for welding P91 steels using conventional arc welding methods [7] call for weld hardness from 240 to 300 HV, which was made by post weld heat treatment at an appropriate temperature, time and cooling rate (usually 760 ^{0}C for minimum two hours and 150-200 ^{0}C/hour). Laser treatment may not require such long time at the temperature to achieve the proper hardness. But methods to control the very short time at temperature and the cooling rate that are basically required for achieving the proper low hardness must be developed. The typical hardness profile of arc welded modified 9Cr-1Mo steel after PWHT is shown in Figure 18, which shows a soft hardness zone in the fine grain HAZ where the Type IV cracking usually occurs. The hardness profile of the laser weld does not show such a soft zone in its HAZ, which may lead to Type IV crack free welds.

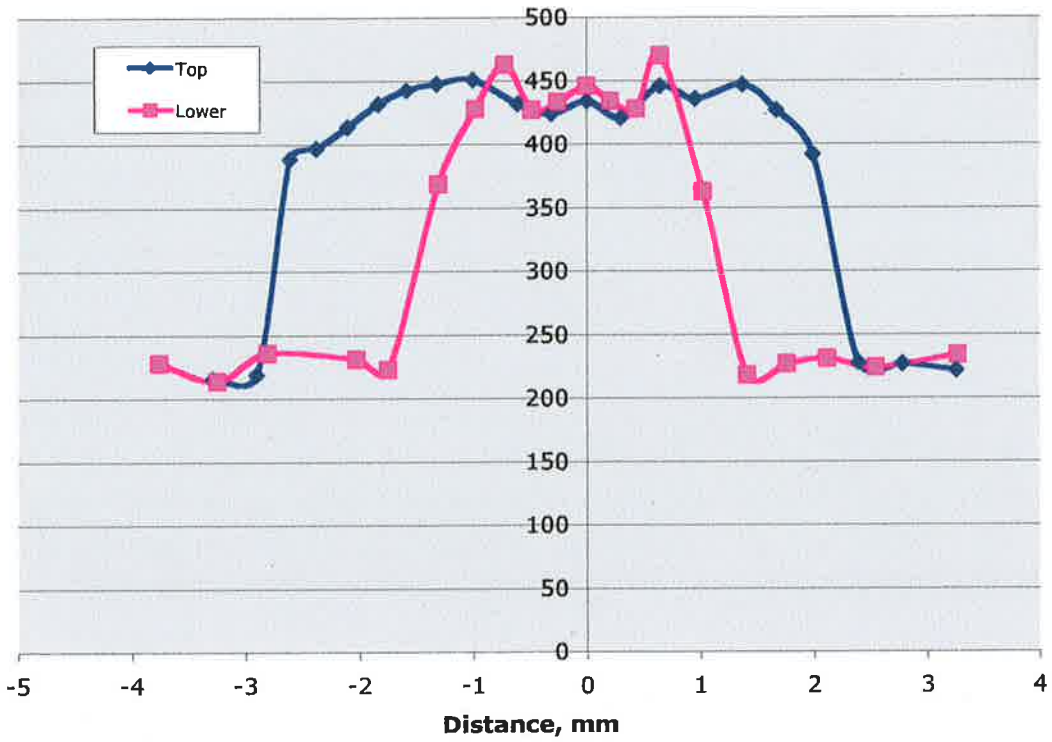

Figure 16. Microhardness profiles of post weld laser treatment (PWLT#1)

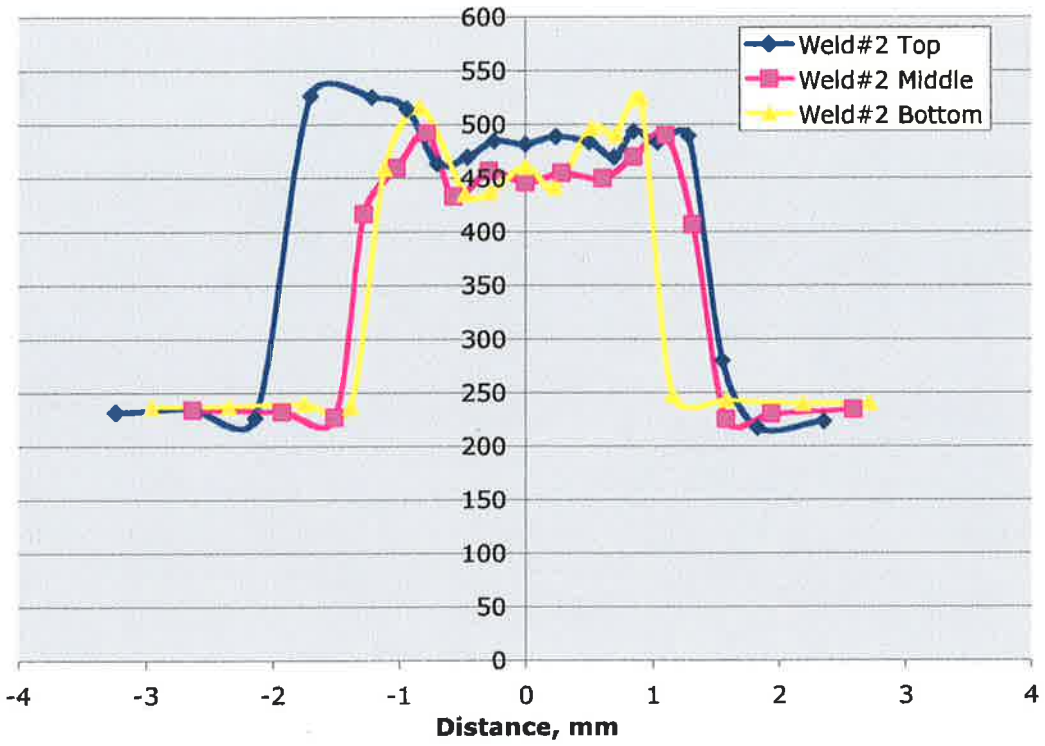

Figure 17. Microhardness profiles of post weld laser treatment (PWLT#2)

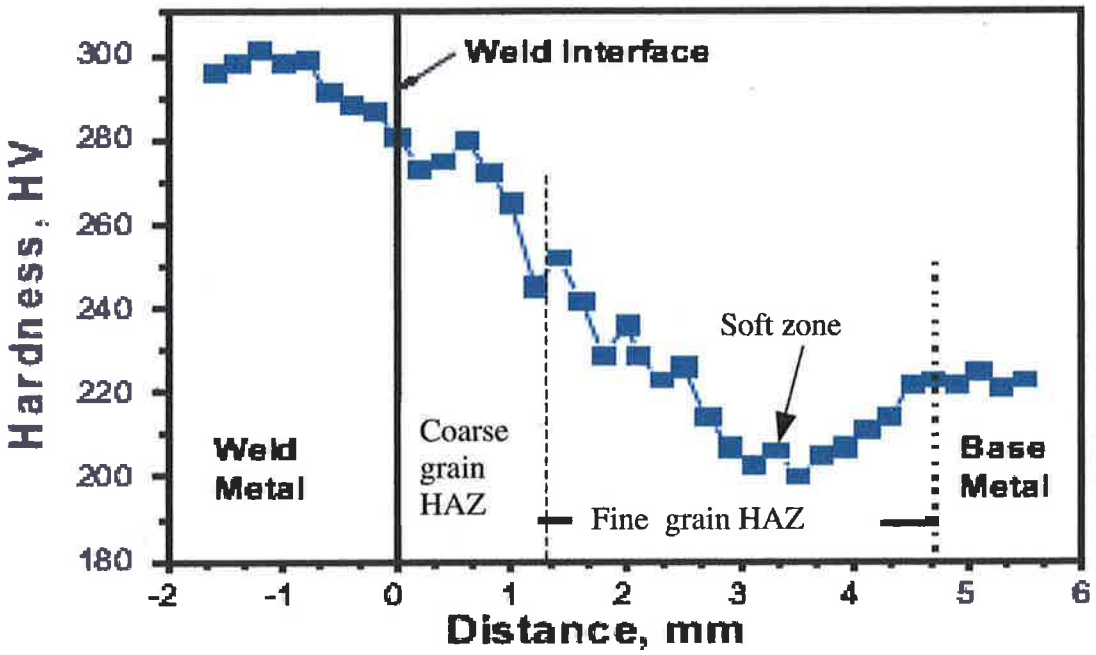

Figure 18. Hardness variation across the weld joint of modified 9 Cr-1Mo steel.

Conclusions

Laser welding and post weld laser treatment of modified 9Cr-1MoVNb steels (Grade P91) were performed in this preliminary study to investigate the feasibility of using a laser welding process as a potential alternative to arc welding methods for solving the Type IV cracking problem in P91 steel welds. The mechanical and metallurgical testing of the laser-welded samples shows the following conclusions:

1. Both bead-on-plate and circumferential butt welds made by a pulsed Nd:YAG laser show good welds that are free of microcracks and porosity. The narrow heat affected zone has a homogeneous grain structure without conventional soft hardness zone where the Type IV cracking occurs in conventional arc welds.
2. The laser weld tests also show that the same laser welder has the potential to be used as a multi-function tool for weld surface remelting, glazing or post weld tempering to reduce the weld surface defects and to increase the cracking resistance and toughness of the welds.
3. The Vickers hardness of laser welds in the weld and heat affected zones was 420 – 500 HV, with peak hardness in the HAZ, compared to 240 HV of base metal. Post weld laser treatment was able to slightly reduce the peak hardness and smoothen the hardness profile, but failed to bring the hardness down to below 300 HV due to insufficient time at temperature and too fast cooling rate after the time. Though optimal hardness of laser welds will be determined based on best weld strength, methods to achieve the post weld laser treatment temperature, time at the temperature, and adequately slow cooling rate still need to be developed.
4. Mechanical testing of the laser welds and post weld laser treated samples, which have not yet been completed, must be performed to evaluate the effects of laser post treatments such as surface remelting, glazing, re-hardening, or tempering on the strength of the welds.

References

1. H. Cerjak and E. Letofsky, *Science and Technology of Welding and Joining*, 1996, 1, (1), pp. 36 – 42.
2. C. Coussement, "New Ferritic/Martensitic Creep Resistant Steel: Promises and Challenges in the New Century," EPRI Conf. On 9Cr Materials Fabrication and Joining Technology, JULY 10-11, 2001, Myrtle Beach, SC.
3. K. Haarmann, et al., "The T91/P91 book", Boulogne, Vallourec & Mannesmann Tubes, 2002.
4. M. Yamazaki, et al., "Creep rupture properties of welded joints of heat resistant steels," J. of Power and Energy Systems, Vol. 2, No. 4, 2008.
5. S. L. Mannan and K. Laha, Trans. Ind. Inst. Met., 1996, 49, (4), 303 – 320.
6. Sperko Engineering, "Welding Grade 91 Alloy Steel", October 2005.
7. K. Coleman and D. Grandy, "Guideline for welding P(T) 91", EPRI Technical Report 1006590, June 2002.

Nuclear Engineering Division
Argonne National Laboratory
9700 South Cass Avenue
Argonne, IL 60439

www.anl.gov

A U.S. Department of Energy laboratory
managed by UChicago Argonne, LLC